

Downloaded from UvA-DARE, the institutional repository of the University of Amsterdam (UvA)
<http://hdl.handle.net/11245/2.28045>

File ID uvapub:28045
Filename 126250y.pdf
Version unknown

SOURCE (OR PART OF THE FOLLOWING SOURCE):

Type article
Title Microscopic structure of Er-related optically active center in crystalline Si
Author(s) N.Q. Vinh, H. Przybylinska, Z.F. Krasil'nik, T. Gregorkiewicz
Faculty FNWI: Van der Waals-Zeeman Institute (WZI)
Year 2003

FULL BIBLIOGRAPHIC DETAILS:

<http://hdl.handle.net/11245/1.215987>

Copyright

It is not permitted to download or to forward/distribute the text or part of it without the consent of the author(s) and/or copyright holder(s), other than for strictly personal, individual use, unless the work is under an open content licence (like Creative Commons).

Microscopic Structure of Er-Related Optically Active Centers in Crystalline Silicon

N. Q. Vinh,¹ H. Przybylińska,² Z. F. Krasil'nik,³ and T. Gregorkiewicz¹

¹*Van der Waals–Zeeman Institute, University of Amsterdam, Valckenierstraat 65, NL-1018 XE Amsterdam, The Netherlands*

²*Institute of Physics, Polish Academy of Sciences, Al. Lotników 32/46, PL-02 668 Warszawa, Poland*

³*Institute for Physics of Microstructures, GSP-105, 603600 Nizhny Novgorod, Russia*

(Received 10 May 2002; published 11 February 2003)

A successful observation and analysis of the Zeeman effect on the $\lambda \approx 1.54 \mu\text{m}$ photoluminescence band in Er-doped crystalline MBE-grown silicon are presented. The symmetry of the dominant optically active centers is conclusively established as orthorhombic $I(C_{2v})$ with $g_{\parallel} \approx 18.39$ and $g_{\perp} \approx 0$. In this way the long standing puzzle as regards the paramagnetism of optically active Er-related centers in silicon is settled. Preferential generation of a single type of an optically active Er-related center confirmed in this study is essential for photonic applications of Si:Er.

DOI: 10.1103/PhysRevLett.90.066401

PACS numbers: 71.70.Ej, 61.72.Tt, 78.66.Db

Rare earth doping of semiconductors is known to result in the formation of luminescent centers suitable for applications in optoelectronic devices [1,2]. Among the various rare earth elements, Er has attracted particular attention because the $4I_{13/2} \rightarrow 4I_{15/2}$ transition involving nonbonding $4f$ shell electrons of the Er^{3+} ion ($4f^{11}$) occurs at the technologically important wavelength of $1.54 \mu\text{m}$, matching the absorption minimum of silica-based optical fibers. The Si:Er system is of special interest in view of the success and versatility of silicon technology. Also, Si:Er light emitting structures are attractive in association with potential applications for optical interconnects in future photonic chip technology. As a result of a continuing research effort Si:Er-based light emitting diodes have now been successfully developed—for an up-to-date review, see, e.g., [3]. A further increase of emission efficiency and thermal stability by materials engineering is, however, obstructed by the apparent lack of understanding of more fundamental aspects related to the optical activity of Er^{3+} ions in Si. In contrast to previously mentioned impressive developments toward practical devices, the Si:Er system remains poorly understood and even controversial as regards the microstructure of the optically active Er-related centers and the relevant energy transfer mechanisms [4]. This situation is all the more unfortunate, when bearing in mind the prominent position of Si:Er with respect to applications.

The microscopic structure of Er dopants in Si has been investigated using extended x-ray-adsorption fine structure, and the presence of oxygen in the immediate surrounding of the optically active Er atom was concluded [5]. The formation of an Er-related cubic center has been found in channeling experiments [6], which identified an isolated Er atom at a tetrahedral interstitial site as the dominant center generated in crystalline silicon by Er implantation. The findings are in accordance with theoretical calculations for isolated Er in Si [7]. Unfortunately, these techniques cannot directly distinguish between optically active and nonactive Er-related centers. Having in mind that only a small percentage (1 to 10%) of

Er dopants in silicon exhibit optical activity [2,8], there exists a large probability that above-mentioned studies concern the nonactive species and therefore are not relevant for the issues related to light emission from Si:Er. Also electron paramagnetic resonance (EPR), the experimental technique for the identification of the microstructure of defects, failed to detect the optically active Er-related centers in crystalline silicon [9]. Microscopic information on centers responsible for Er-related $1.5 \mu\text{m}$ emission in Si was revealed by high-resolution photoluminescence (PL) study which identified more than 100 emission lines related to several Er-induced centers [8].

Microscopic aspects of the Er-related emitting center would best be provided by the magneto-optical study of the main features of the emission spectrum. However, due to the inhomogeneous character of PL bands, application of magnetic field results in broadening and thus subsequent vanishing of the emission lines. Consequently, in spite of repeated claims [10], no successful observation of Zeeman effect in PL has been reported for Si:Er until now. The situation is dramatically different for Si:Er material grown recently by the sublimation MBE technique. In this case, the PL spectrum (depicted in Fig. 1) contains only a few lines of a very small width $\Delta E < 10 \mu\text{eV}$. Based on crystal field analysis, there were assigned for a single type of center, labeled Er-1, of non-cubic symmetry [11]. Taking advantage of the small linewidth of the Er-1 spectrum a successful observation of Zeeman effect in PL was possible. In this Letter we present results of the magneto-optical investigation of the main PL band ($\lambda \approx 1.54 \mu\text{m}$) of the Er-1 spectrum, indicated with an arrow in Fig. 1. We note that also the (broad) PL spectra observed in Er-implanted samples usually have maxima located at this wavelength [3,8]. Consequently, our findings are important for understanding of the optical activity of Si:Er in general.

The inset to Fig. 1 shows a cartoon of the structure used in the current study. It comprises 400 interchanged Si and Si:Er layers of a few nanometers thickness stacked along

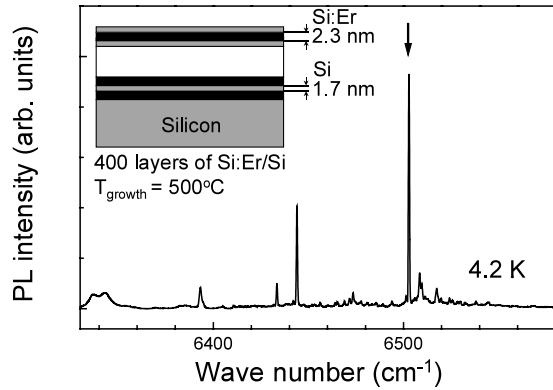


FIG. 1. Photoluminescence spectra of the multilayer Si/Si:Er structure used in the current study (see inset), as measured at $T = 4.2$ K. The arrow marks the most intense emission line for which the Zeeman effect was subsequently investigated.

the $\langle 100 \rangle$ growth direction. Magneto-optical experiments were performed at 4.2 K using a cw Ar^+ -ion laser operating at 514.5 nm for excitation. The sample was placed in a split-coil superconducting magnet with optical access. The emerging luminescence was dispersed by a high-resolution 1.5 m $f/12$ monochromator (Jobin Yvon THR-1500 equipped with a 600 grooves/mm grating blazed at 1.5 μm), and detected with a liquid-nitrogen cooled Ge detector (Edinburgh Instruments). For polarization measurements a quarter-lambda plate and a linear polarization filter were used.

In the tetrahedral environment the $4I_{13/2}$ first excited state of the $4f^{11}$ shell of the Er^{3+} ion splits into a series of $2\Gamma_6 + \Gamma_7 + 2\Gamma_8$ sublevels and the ground $4I_{15/2}$ state splits into the sequence $\Gamma_6 + \Gamma_7 + 3\Gamma_8$ [12]. Consequently, at low temperatures five PL lines are expected. A lower symmetry crystal field splits the remaining quartets into doublets. In this case eight spectral components will appear, with each PL line corresponding to a transition between effective spin doublets. Application of a magnetic field splits the doublets further due to the Zeeman effect, in a pattern reflecting the symmetry of the Er^{3+} -related optically active center. The Hamiltonian describing the Zeeman splitting is given by

$$\mathcal{H} = \mu_B \mathbf{B} \cdot \mathbf{g} \cdot \mathbf{S}, \quad (1)$$

with $\mathbf{S} = 1/2$, μ_B being the Bohr magneton, and the effective \mathbf{g} tensor exhibiting the symmetry of the center. In general, every PL line corresponding to a transition between two doublets will split into four components, with $\Delta E = \pm 1/2(|\mathbf{G} - \mathbf{g}|)\beta\mathbf{B}$ for $\Delta M_S = 0$ transitions and $\Delta E = \pm 1/2(|\mathbf{G} + \mathbf{g}|)\beta\mathbf{B}$ for $\Delta M_S = \pm 1$ transitions, where \mathbf{G} and \mathbf{g} are the effective g tensors of the upper and lower doublets, respectively. The magnetic dipole allowed $\Delta M_S = \pm 1$ transitions to have a very low probability and for the rare earths usually only electric dipole allowed transitions with $\Delta M_S = 0$ are observed. In the present study none of the emission components appearing upon

application of magnetic field was circularly polarized, which means that only the $\Delta M_S = 0$ transitions are observed. Figure 2 shows the Zeeman effect for the PL line indicated with an arrow in Fig. 1. In magnetic fields of up to 5.25 T, the splitting into three components for $\mathbf{B} \parallel \langle 100 \rangle$ and seven components for $\mathbf{B} \parallel \langle 011 \rangle$ can be concluded.

Keeping the magnetic field fixed at 5.25 T and rotating its direction in the (011) and (100) planes, we observe a pronounced angular dependence of the line positions. This tells us that the symmetry of the optically active center is lower than cubic. Figure 3(a) shows the positions of PL bands for the magnetic field rotated in the (011) plane. As can be concluded, the center has four non-equivalent orientations for an arbitrary direction of \mathbf{B} . The position of one of them is nearly constant for all field orientations — for this line the effective g factors of the upper and lower states must be almost equal. Although the angular dependence is complicated by anticrossings among the sublevels, it can be clearly concluded that the center possesses orthorhombic $I(C_{2v})$ symmetry. For this symmetry type, two of the main tensor axes are oriented along the nonequivalent $\langle 011 \rangle$ directions, taken as x and y , while the z axis is the $\langle 100 \rangle$ oriented intersection of the planes perpendicular to x and y . In this Letter, we adopt a

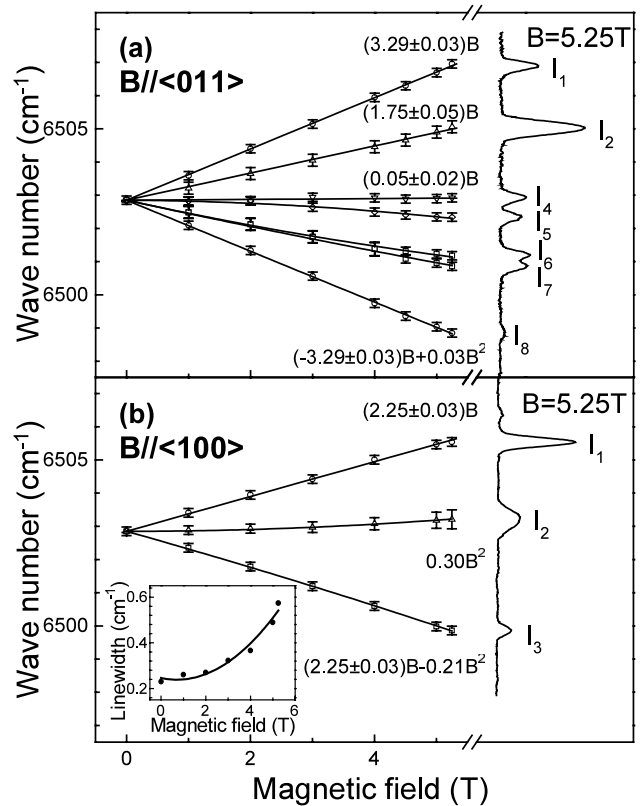


FIG. 2. Magnetic field induced splitting of the main PL line at $T = 4.2$ K for (a) $\mathbf{B} \parallel \langle 011 \rangle$ and (b) $\mathbf{B} \parallel \langle 100 \rangle$. In the inset, the linewidth of the I_2 component is shown as a function of magnetic field.

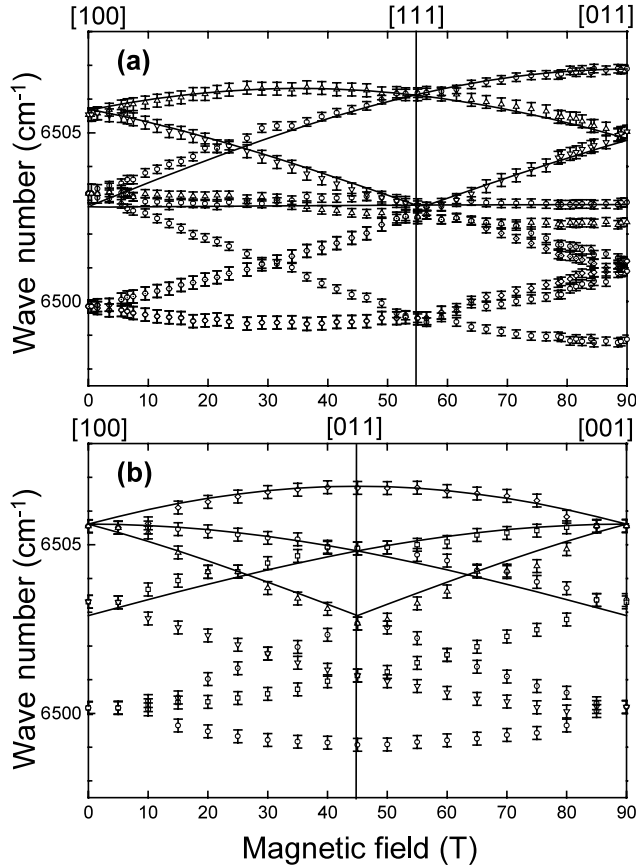


FIG. 3. Angular dependence of the Zeeman effect of the main PL line (marked with an arrow in Fig. 1) at $B = 5.25$ T for (a) the (011) and (b) the (100) crystallographic planes. Solid lines correspond to simulations—see text for the further explanation.

description where the spin quantization z axis is chosen along the tensor axis with the greatest g value, in this case one of the $\langle 011 \rangle$ directions.

It is important to check whether the particular form of the sample, a $\langle 100 \rangle$ -grown stack, has no influence on the local symmetry of the Er-related center responsible for the observed emission. Figure 3(b) illustrates the positions of PL bands split by the magnetic field rotated in the (100) plane, from the $\langle 100 \rangle$ direction perpendicular to the sample surface (the growth direction), through the $\langle 011 \rangle$, and again to the $\langle 100 \rangle$, but now within the plane of the sample. As can be seen, the observed pattern is fully symmetric within the 90° rotation. We conclude that the layer stacking procedure and the thin-layer form of the sample do not affect the symmetry of the Er-related optically active center, thus making the results of the present study relevant for the Si:Er system in general.

A closer inspection of the angular dependencies in Fig. 3 reveals that the splitting towards higher and lower emission energies is not symmetric. This is due to the fact that at high magnetic fields the magnitude of the Zeeman splitting becomes comparable with the crystal field effect

and therefore mixing between individual sublevels in the $J = 15/2$ and $J = 13/2$ manifolds appears. In the particular case of the investigated PL line, only transitions from lower lying level of the excited state doublet to the lower lying level of the ground state doublet will be unaffected, since these are not disturbed by the presence of other Er-related levels. In contrast, other lines will show higher order contributions in B , complicating the pattern. The transitions occurring from the lower level of the Zeeman split lowest doublet of the excited state are easily identified since their intensity is higher due to partial thermalization. As can be seen from Fig. 2, more intense lines occur at higher energies, which thus give us the additional information that $|\mathbf{G}| < |\mathbf{g}|$.

The values of the effective g tensor $\mathbf{g}_{\text{eff}} = |\mathbf{g} - \mathbf{G}|$ can be determined from the Zeeman splitting shown in Fig. 2. For $\mathbf{B} \parallel \langle 011 \rangle$ —Fig. 2(a)—we get $\Delta g_z = |g_z - G_z| = 3.29 \pm 0.03$. This value is determined quite accurately since for \mathbf{B} oriented along the z tensor axis there are no anticrossing effects. For the components related to Δg_y [I_4 and I_5 lines in Fig. 2(a)], the relative intensity of line I_4 does not change with magnetic field and the peak position stays constant, whereas the lower one (I_5) shifts towards lower energy as B^2 . The Δg_y value estimated from the linear part of the splitting is less than 0.05. For the central branch [I_2 in Fig. 2(a)], we obtain $g_{\text{eff}} = 1.75 \pm 0.05$. This value is much less accurate as we are in fact dealing with two superposed branches, as can be seen by the growth of the linewidth with increasing B , especially for the lower-energy component for which second order effects are considerable. The lowest accuracy is obtained with $\mathbf{B} \parallel \langle 100 \rangle$ [Fig. 2(b)]: the central line broadens strongly with \mathbf{B} but does not split. The inset to Fig. 2(b) shows that the dependence of the linewidth on magnetic field for the central line is not linear with \mathbf{B} . When rotating magnetic field out of the main direction $\langle 100 \rangle$, this feature splits into four lines, of which two do not change with magnetic field, i.e., $\Delta g_x = 0$. We therefore conclude that the angular dependence shown in Fig. 3 can be described with the following effective g tensor $\Delta \mathbf{g} = |\mathbf{g} - \mathbf{G}| = [0 \pm 0.02, 0.05 \pm 0.02, 3.29 \pm 0.03]$. As can be seen from the solid lines in Fig. 3, simulation with the Hamiltonian (1) gives in this case good agreement with the experimental data.

Unfortunately, one cannot use angular dependencies depicted in Fig. 3 to determine the individual g tensors of the upper and lower doublets \mathbf{g} and \mathbf{G} . Assuming full thermalization, these can be estimated from the temperature dependence of the intensity ratio of the high and the low energy components at high field. We note that the components I_1 for $\mathbf{B} \parallel \langle 100 \rangle$ and $\mathbf{B} \parallel \langle 011 \rangle$ increase in intensity with magnetic field, while components I_3 and I_8 for $\mathbf{B} \parallel \langle 100 \rangle$ and $\mathbf{B} \parallel \langle 011 \rangle$, respectively, decrease due to thermalization within the upper doublet. The intensity ratio of these components follows a Boltzmann's distribution, with the activation energy equal to the splitting

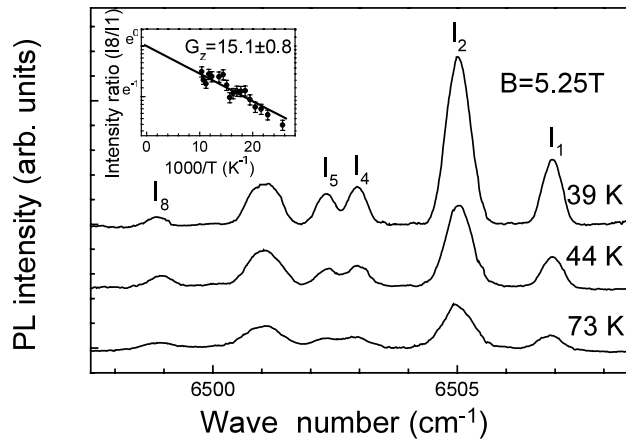


FIG. 4. Magnetic field induced splitting of the main PL line for $B = 5.25$ T, $\mathbf{B}||\langle 011 \rangle$ at temperatures of $T = 39, 44,$ and 73 K. The inset shows the intensity ratio I_8/I_1 fitted assuming thermalization within the upper doublet.

within the upper doublet. The PL spectra for $B = 5.25$ T and $\mathbf{B}||\langle 011 \rangle$ at $T = 39, 44,$ and 73 K are illustrated in Fig. 4. As shown in the inset to the figure, the temperature dependence of individual PL components allows an estimate of $|G_z| \cong 15.1 \pm 0.8$ to be made (this is done for a higher temperature range $T \geq 40$ K, in order to assure full thermalization [13]). The intensity ratio of two components related to $\Delta g_y = 0.05(I_4, I_5)$ is not changing with temperature indicating $|G_y| \cong 0$. For components corresponding to $\Delta g_x \cong 0$ at $\mathbf{B}||\langle 100 \rangle$, the central line does not split with magnetic field. We notice that the line remains fully symmetric upon increasing temperature, so that also $|G_x| \cong 0$. Therefore both $|G_x|$ and $|G_y|$ are very small: i.e., the $|G_\perp|$ value for the excited state is close to zero. Hence, we are dealing with a particular situation where $|g_\perp|$ is close to zero for both the ground and the excited state doublets. This gives us the \mathbf{g} tensor for the ground state doublet $g_{||} \cong 18.39 \pm 0.81$ and $g_\perp \cong 0$, and results in trace of $\text{Tr}(\mathbf{g}) \cong 18.4 \pm 1.5$. The fact that $g_\perp \cong 0$ implies a low probability of spin transitions within the ground state. This result provides an explanation as to why the Er^{3+} -related optically active centers in crystalline silicon have not been detected using magnetic resonance. The situation is similar to that treated by Watkins *et al.* [14] for Au dopant in Si. (When $g_\perp \cong 0$, there are no magnetic field dependent off-diagonal terms and no $\Delta m = \pm 1$ transitions can be induced by microwave field.)

If only small axial distortions are present, the average g_{av} factor can be related to the isotropic cubic g_c factor [15] $g_{\text{av}} = g_c = \frac{1}{3}(g_{||} + 2g_\perp)$. In the present case the average g_{av} value as defined by is 6.13 ± 0.5 , similar as found for Er in different host materials [9,16,15]. For isotropic centers the g tensors of Γ_6 and Γ_7 are 6.8 and 6.0, respectively [16,15]. Therefore in the present case the ground state is likely to be of a Γ_6 character, which is in

agreement with the previous interpretation of experimental data [8,9]. The observed orthorhombic I symmetry is likely to arise from a distortion of a tetrahedrally coordinated Er^{3+} ion. This was also recently considered in total energy calculations for the most stable configuration of Er^{3+} ion in the crystalline silicon host [17].

In summary, we have provided the most direct microscopic information on the structure of a prominent center responsible for optical activity of Er in crystalline silicon. From a clear Zeeman effect observed on the main line of the Er-1 PL spectrum, the lower than cubic symmetry of the emitting center is confirmed and conclusively identified as orthorhombic I (C_{2v}) with \mathbf{g} tensor of the ground state $g_{||} \cong 18.39 \pm 0.81$, $g_\perp \cong 0$. On the basis of these findings, the paramagnetism of the Er^{3+} -related center emitting at $\lambda \approx 1.5 \mu\text{m}$ is unambiguously established, and our understanding of the important and notoriously difficult Si:Er system has been significantly advanced.

We note that the preferential formation of one type of Er-related optically active center, as confirmed by the success of the reported Zeeman effect study, is a necessary prerequisite for development of efficient photonic devices based on Si:Er.

The work was financially supported by the *Nederlandse Organisatie voor Wetenschappelijk Onderzoek* (NWO) and the *European Research Office* (ERO). The authors are grateful to M. S. Golden for a critical reading of the manuscript.

-
- [1] S. S. Iyer and Y. H. Xie, *Science* **260**, 280 (1993); S. Schmitt-Rink *et al.*, *Phys. Rev. Lett.* **66**, 2782 (1991).
 - [2] A. Polman, *J. Appl. Phys.* **82**, 1 (1997).
 - [3] S. Coffa *et al.*, *Mater. Res. Bull.* **23**, 25 (1998).
 - [4] J. Palm *et al.*, *Phys. Rev. B* **54**, 17603 (1996).
 - [5] D. L. Adler *et al.*, *Appl. Phys. Lett.* **61**, 2181 (1992).
 - [6] U. Wahl *et al.*, *Phys. Rev. Lett.* **79**, 2069 (1997).
 - [7] M. Needels *et al.*, *Phys. Rev. B* **47**, 15 533 (1993).
 - [8] H. Przybylińska *et al.*, *Phys. Rev. B* **54**, 2532 (1996).
 - [9] J. D. Carey *et al.*, *Phys. Rev. B* **59**, 2773 (1999).
 - [10] Observation of Zeeman effect in PL of Si:Er was claimed in several abstracts submitted to meetings devoted to defects in solids (MRS, ICDS).
 - [11] B. A. Andreev *et al.*, *J. Cryst. Growth* **201/202**, 534 (1999); M. V. Stepihova *et al.*, *Thin Solid Films* **369**, 426 (2000).
 - [12] K. R. Lea *et al.*, *J. Phys. Chem. Solids* **23**, 1381 (1962).
 - [13] N. Q. Vinh *et al.*, *Physica (Amsterdam)* **308B–310B**, 340 (2001).
 - [14] G. D. Watkins *et al.*, *Phys. Rev. Lett.* **67**, 1149 (1991).
 - [15] R. K. Watts and W. C. Holton, *Phys. Rev.* **173**, 417 (1968).
 - [16] J. D. Kingsley and M. Aven, *Phys. Rev.* **155**, 235 (1967).
 - [17] A. G. Raffa and P. Ballone, *Phys. Rev. B* **65**, 121309 (2002).